

LIGO Laboratory / LIGO Scientific Collaboration

LIGO- T0900447-v4

ADVANCED LIGO

24th Feb 2014

Final Design Document ETM/ITM ears

**M. van Veggel, A. Bell, A. Cumming, L. Cunningham, G. Hammond, K. Haughian, J. Hough,
R. Jones, R. Kumar, K. Strain, S. Rowan**

Institute for Gravitational Research, University of Glasgow

Distribution of this document:
LIGO Science Collaboration.
This is an internal working note
of the LIGO Project.

California Institute of Technology
LIGO Project – MS 18-34
1200 E. California Blvd.
Pasadena, CA 91125
Phone (626) 395-2129
Fax (626) 304-9834
E-mail: info@ligo.caltech.edu

LIGO Hanford Observatory
P.O. Box 1970
Mail Stop S9-02
Richland WA 99352
Phone 509-372-8106
Fax 509-372-8137

**Institute for Gravitational
Research**
University of Glasgow
Kelvin Building
Glasgow G12 8QQ
Phone: +44 (0)141 330 3340
Fax: +44 (0)141 330 6833
Web: www.physics.gla.ac.uk/igr/

Massachusetts Institute of Technology
LIGO Project – NW22-295
185 Albany St
Cambridge, MA 02139
Phone (617) 253-4824
Fax (617) 253-7014
E-mail: info@ligo.mit.edu

LIGO Livingston Observatory
P.O. Box 940
Livingston, LA 70754
Phone 225-686-3100
Fax 225-686-7189

<http://www.ligo.caltech.edu>

1 Table of contents

1	<i>Table of contents</i>	2
1.1	Revision history	3
1.2	Reference documents	3
1.3	Acronyms	4
2	<i>Introduction</i>	5
2.1	Overview of the monolithic final stage	5
2.2	Design requirements for the ears	6
2.3	Structure of the document	7
3	<i>Design description and analyses</i>	8
3.1	Shape of the ears	8
3.2	Stresses	8
3.2.1	Hand calculations and arguments on stress	8
3.2.2	Finite element analysis under nominal load	9
3.2.3	Finite element analysis of ears with a misalignment of the fibres	12
3.3	Weldability	14
3.4	Location of the ear and suspension dynamics	15
3.5	Hydroxide catalysis bonding	17
3.6	Thermal noise of the bonds	17
3.7	Thermal Noise contribution from material loss of the fibres	18
4	<i>Fabrication procedure</i>	19
4.1	Shaping of the ear	19
4.2	Flame polishing	21
4.3	Polishing of the bonding surface	21
5	<i>Tests performed</i>	22
5.1	Hydroxide catalysis bonding	22
5.2	Weldability and strength tests	22
5.2.1	Welding procedure	22
5.2.2	Double fibre cartridge tests	23
5.2.3	Full test suspensions	24
5.2.4	Bond quality	25
5.2.5	Weld horns	25
6	<i>Conclusions</i>	27
	<i>Appendix 1</i>	28

1.1 Revision history

Rev v1	2 nd November 2009	Posted for fabrication readiness review (M. van Veggel)
Rev v2	3 rd November 2009	Revisions after comments N. Robertson (M. van Veggel)
Rev v3	15 th December 2009	Minor changes (M. van Veggel)
Rev v4	24 th Feb 2014	Added section on “crackle” in section 3.6 (Norna A Robertson, wording from Glasgow group)

1.2 Reference documents

<i>Design documentation of the “ears”</i>	
D080751-02-K	ETM/ITM test mass ear
D090007-00-K	ETM/ITM penultimate mass ear
<i>Analysis documentation</i>	
P0900084-v2	Finite element modeling of the mechanical loss of silica suspension fibres for advanced gravitational wave detectors
P0900053-v2	Thermal noise arising from bonds in the Advanced LIGO test mass suspensions
<i>Back ground documentation</i>	
T080338-v1	Ear redesign progress presented 21/11/2008
G0900108	Update on monolithic suspension work
G0900783	Update on monolithic suspension work Glasgow and MIT
T0900391	Monolithic suspension procedure
T010075-01	Advanced LIGO systems design
G0900507-v2	Overview of monolithic suspension work in Glasgow
T080096-v1	Wire attachment points and flexure corrections
T070138-01	Ribbon/Fibre length budget
M080134	ETM/ITM and BS/FM pitch frequencies and d-values
T080343-00	Collated strength data for Hydroxide Catalysis Bonds
M060056-10	Advanced LIGO Reference Design
T0900556-v1	Note on revision of monolithic quad pendulum “d” parameters to enable revised ears and welding
T0900557-v1	NP-type monolithic suspension: testing record of the ears
T080091-00	Proposal for baseline change from ribbons to fibres in AdvLIGO test mass suspension monolithic stage
<i>Publications</i>	

Class. Quant. Grav. 19 (2002) 1655-1662	Barr et al. <i>Silica Research in Glasgow</i>
Class. Quant. Grav. 22 (2005) S257–S267	Elliffe et al. <i>Hydroxide-catalysis bonding for stable optical systems for space</i>

1.3 Acronyms

ETM End Test Mass

ITM Input Test Mass

PUM Penultimate Mass

COM Centre of Mass

2 Introduction

This document serves as the final design document for the fabrication readiness review of specifically the “ears” that are attached using hydroxide catalysis bonding to the sides of the ETM and ITM masses for the monolithic final stage of the quadrupole suspension in Advanced LIGO.

The document discusses and refers to the design, the fabrication procedure, the analyses performed during design, the method of attachment to the ETM/ITM test masses and penultimate masses and tests performed on the test batch of ears to prove fabrication readiness.

2.1 Overview of the monolithic final stage

The input and end test masses (ITM and ETM) for advanced LIGO will be suspended using a quadruple suspension system in which the final stage consists of a penultimate mass (PUM) connected monolithically via silica fibres and “ears” to the ETM or ITM as shown in Figure 2.1.

The ears are connected to the ETM/ITM test masses and to the ETM/ITM PUM’s through hydroxide catalysis bonding (M060056-10 p. 16).

The fibres are pulled from 3 mm diameter Suprasil 2 stock using a CO₂ laser. The baseline is that the fibre ends are laser welded onto the ears (M060056-10 p. 16).

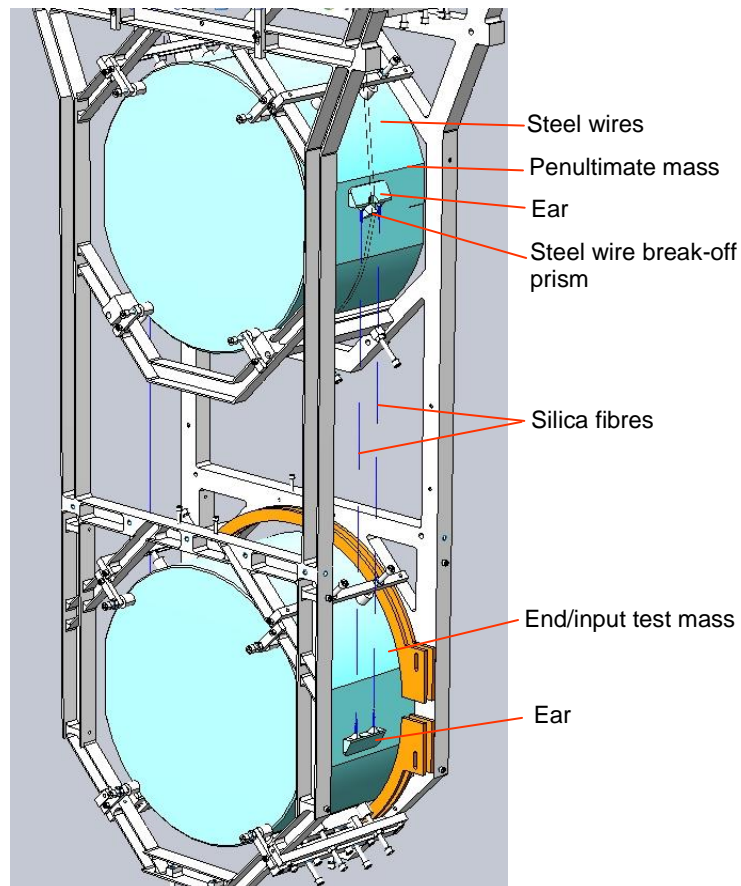


Figure 2.1 Final monolithic stage of the quadrupole suspension of the ETM/ITM

2.2 Design requirements for the ears

The most basic requirements of the ears are:

- The ears shall be made of Suprasil 312.
- The ears are a strong interface between the mass and the fibres with a sufficiently large safety factor. The nominal stresses should not exceed 1/3 of the maximum tensile strength of silica.
- The thermal noise level for a single Adv LIGO mass due to the ears and bonds at 100 Hz has to be less than 7×10^{-22} m/ $\sqrt{\text{Hz}}$ (as set in T010075-01)
- It must be possible to weld the fibres to the ears.
- The location of the ears should not interfere with any other components in the suspension and in combination with the fibres it should be possible to meet the required suspension dynamics (T010075-01, M080134).
- The ears must be manufacturable.

Additional requirements set during the design process:

- The design of the ear should be similar to the proven GEO ear design with butt weld areas [Barr et al. 2002]. The GEO ear consists of one body with 2 weld horns (Figure 2.2). A fibre is butt welded onto each weld horn.

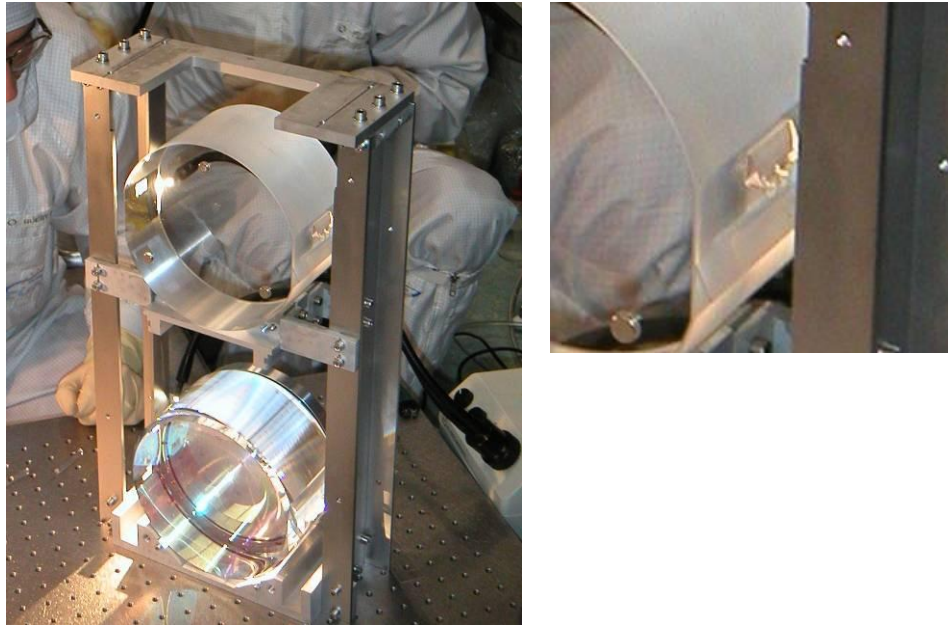


Figure 2.2 Zoom in on a GEO ear during installation in GEO (2004)

- The thermo-elastic noise in the fibres and welds should meet the baseline thermo-elastic noise (T080091-00).
- The nominal bond shear stress of the Advanced LIGO ears should not exceed the nominal shear stress in the GEO ears, i.e. 0.16 MPa (see results in Table 2.1).

The nominal shear stress is given by:

$$\tau_{ear} = \frac{g \cdot m}{n \cdot A}$$

Where,

g gravitational constant [9.81 m/s²]

m mass of the test optic [kg]

n number of ears per mass [-]

A bond area per ear [m²]

Table 2.1 Calculation of the nominal shear stress per ear for GEO and Advanced LIGO

Experiment	Mass of test optic m [kg]	Number of ears n	Bond area A [$\times 10^{-6}$ m ²]	Nominal shear stress per ear τ_{ear} [MPa]
GEO	10	2	$10 \times 30 = 300$	0.16
Advanced LIGO	40	2	$20 \times 60 = 1200$	0.16

2.3 Structure of the document

In section 3 the design of the ear will be discussed following the criteria stated in section 2.2. In section 4 the fabrication procedure will be discussed. In section 5 tests performed on a test batch of 60 ears will be discussed. The document will end with a summary.

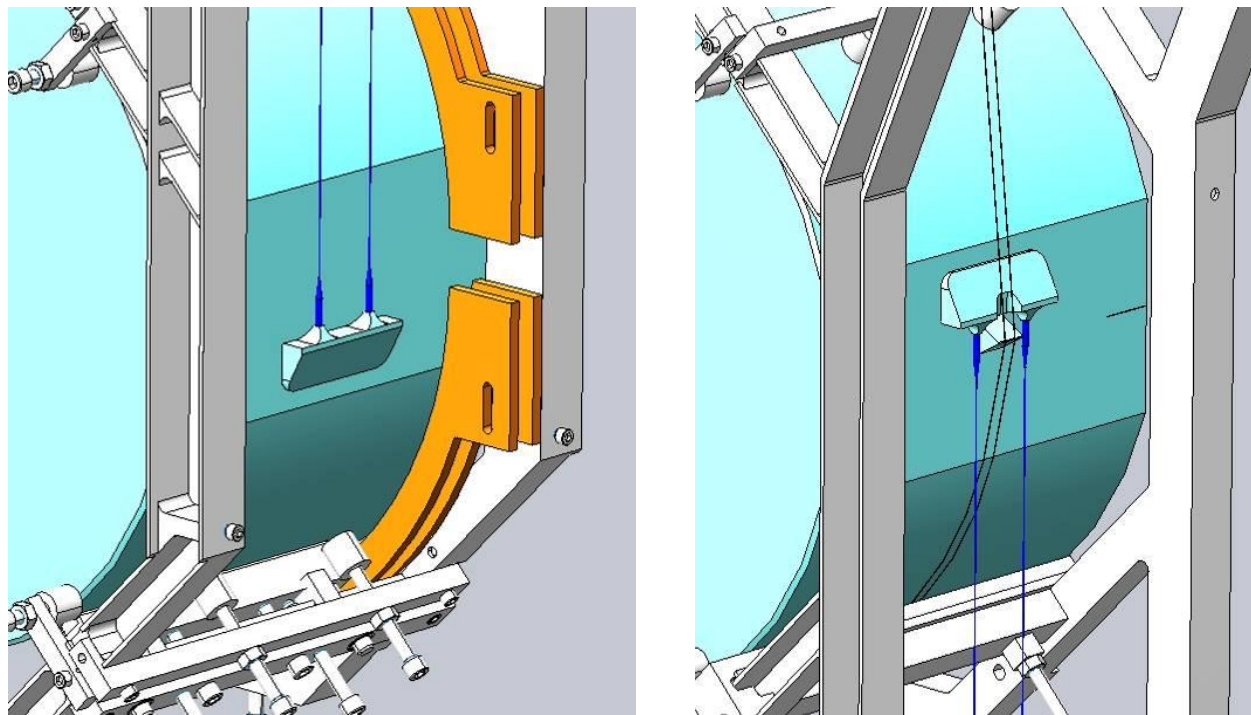
3 Design description and analyses

3.1 Shape of the ears

The shape of the ears is based on the proven ears designed for GEO (compare Figure 2.2 and Figure 3.1). The bond area has been made such that the nominal shear stress is the same for these ears and the GEO ears. Because the mass of the mirrors is 4 times the mass of the GEO mirrors, the bond area has been scaled up by a factor 4, from 10 x 30 mm to 20 x 60 mm. The nominal shear stress is therefore 0.16 MPa. The Ansys FE analysis of this is discussed in the next paragraph.

The required suspension dynamics state that the distance between the fibres should be 30 mm. Therefore the two weld horns are spaced 30 mm apart. The 15 mm on either side of each of the weld horns, allows for symmetrical loading conditions. This limits deformation in the form of bending of the ear weld horns towards the mass as much as possible.

The ears on the penultimate mass are not to interfere with the steel suspension wires, which is why a cut-out has been made into the ear for the PUM.



a) ear on the ITM/ETM

b) ear on the ITM/ETM PUM

Figure 3.1 Zoom in on the ears on the sides of the ITM/ETM and PUM

3.2 Stresses

3.2.1 Hand calculations and arguments on stress

The aim was to minimise bending of the ear weld horns towards the mass as this would produce large differences in stress across the ear. Also, brittle materials like fused silica are more capable of

withstanding compressive stresses than tensile or bending stresses. In compression bulk fused silica can typically withstand a load over 150 MPa, whereas the bulk bending or tensile strength is approximately 50 MPa.

As a brittle material the strength of a silica part is also very sensitive to high stresses at locations where small defects are likely to be, e.g. in edges.

The weld horns necessarily will be subject to large tensile stresses as the fibres are butt-welded onto these. Through welding experiments it was discovered that the smaller the diameter of the stock and the tip of the weld horn, the easier it was to create laser welds. Stock with a diameter of 5 mm was too large to weld well. Stock with a diameter of 2 mm was very easy to weld and good fibres could be pulled from it. However, when calculating the tensile stresses of 2 mm stock in the weld region, one finds a stress of 31.8 MPa using the following equation:

$$\sigma_{tensile} = \frac{F}{A} = \frac{F}{\frac{\pi}{4} \cdot d^2} \quad 3.1$$

where,

- F force on each fibre [N];
- A cross-section area [m²];
- d diameter of the stock [m].

This stress is below the average maximum tensile strength of fused silica, but with a very marginal safety factor of 1.6. It was therefore decided to use 3 mm diameter stock which was still fairly easy to weld and the tensile stress in the welding area would be 14.1 MPa, which means the safety factor is pushed up to 3.5. The tip of the ear has a square profile for manufacturability reasons of 3 x 3 mm, which matches the 3 mm diameter stock.

To make sure the tensile stresses were transferred into the ear by a minimal amount the weld horns were made in a shape approximating a pyramid with a much broader base at the connection to the rest of the ear, such that stresses in the base were much lower. The length of the horn was made as short as possible to allow for this reduction in stress and minimise bending in as short a distance as possible, while still maintaining weldability and manufacturability of the ear. The length of the horn is therefore 6 mm. The base is approximately 11 x 12 mm.

Finally, the aim was to make stresses in the bond area as uniform as possible.

3.2.2 Finite element analysis under nominal load

The design of the ears was analysed using Finite Element analysis. The ears were analysed for the nominal load exerted on them, when fibres are welded to them, which means the ears are fixed in all degrees of freedom on the bonding surface and are subjected to 100 N tensile load in the x-direction on each of the ends of the weld horns as shown in Figure 3.2.

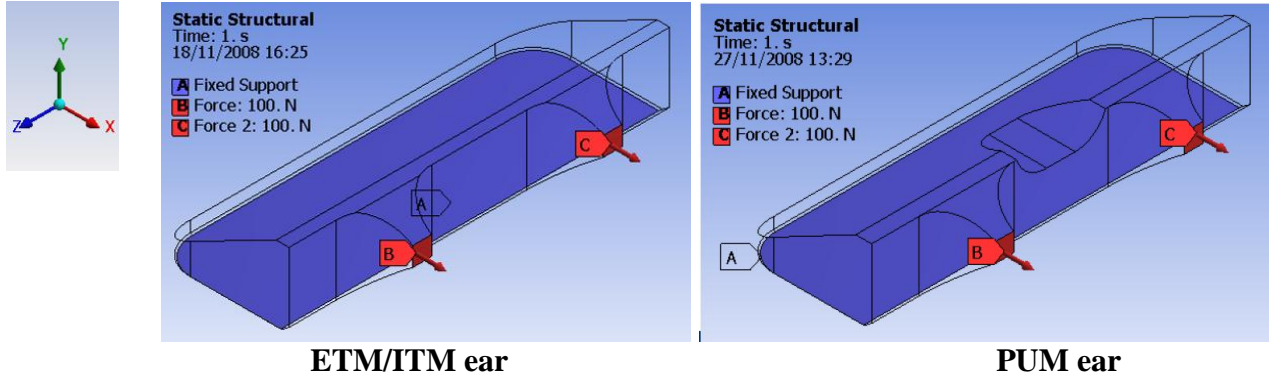
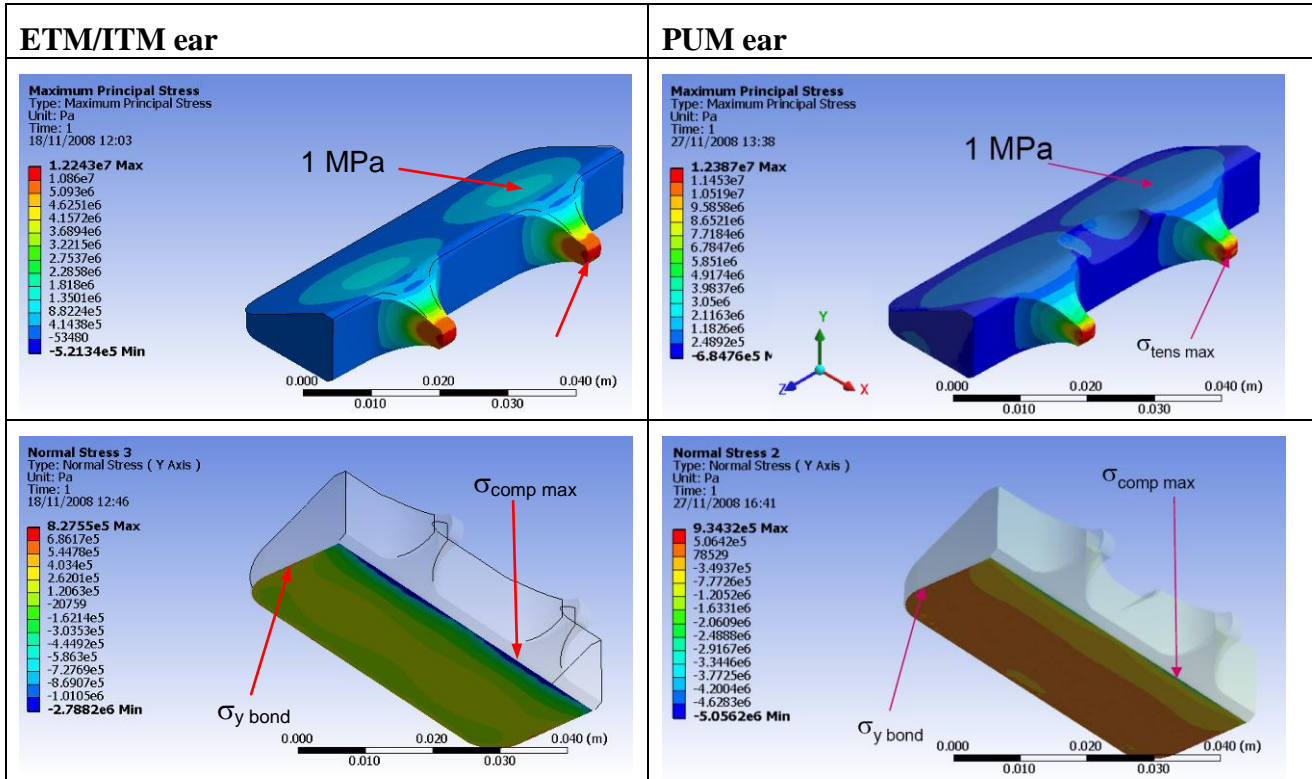


Figure 3.2 Load case for analysis of ears under nominal load

The models were meshed with a sufficiently fine mesh (approximately 65000 elements) and then different stresses and deformation of the ears were analysed. A selection of these is shown in Figure 3.3 and Table 3.1.



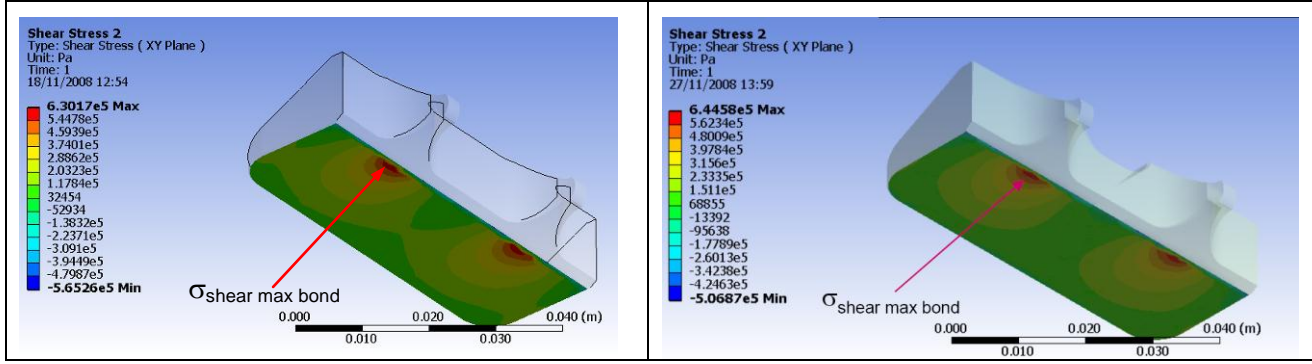


Figure 3.3 Several different stresses for both types of ears

As expected the largest amount of deformation is in the x-direction (the direction in which the load on the fibres is applied). The maximum tensile stress in the weld horn approximates the expected stress of 14.1 MPa closely and is slightly smaller because of the slightly larger square cross-section. From Table 3.1 can be seen that the deformation in y-direction (direction perpendicular to the bonding surface) is about 43% of the deformation in the x-direction which means that bending has not been prevented entirely. It has been minimised though making the horns as symmetrical as possible in y-direction.

The maximum deformation in z-direction is due to the contraction of the weld horns. When comparing the stresses between the ETM/ITM ears and PUM ears it can be seen that the tensile stress and maximum compressive stress rise somewhat for the PUM ears, which is attributed to the slightly reduced stiffness in y-direction of the main body of the ear. There is no reason for concern as stresses are well below 50 MPa (including the compressive stresses).

If a hand calculation is made of the expected shear stress in the xy-plane using equation 2.2, one would find a maximum stress of 0.17 MPa

$$\tau = \frac{2F}{A_{bond}} \tag{3.2}$$

Where,

F force on each weld horn (100) [N]

A_{bond} bond area (20 x 60 mm) [m²].

In Table 3.1 shows however that the maximum shear stress is 0.8 MPa and 0.9 MPa for the ETM/ITM ear and PUM ear respectively. This is because the shear stress is not uniform and is higher around the edges due to a reduced stiffness of the parts, because less material is around. The variation of the shear stresses is limited to a factor 5 from the nominal shear load and is well below the average strength of hydroxide catalysis bonds.

Table 3.1 Several numerical results for both types of ears

Ear	ETM/ITM ear	PUM ear
dx_{max} [mm]	0.7	0.7
dy_{max} [mm]	0.3	0.3
dz_{max} [mm]	0.04	0.04

$\sigma_{tens\ max}$ [MPa]	12.2	12.4
$\sigma_{comp\ max}$ [MPa]	2.8	5.2
$\sigma_{shear\ max\ bond}$ [MPa]	0.6	0.6
$\sigma_{y\ bond}$ [MPa]	0.8	0.9

3.2.3 Finite element analysis of ears with a misalignment of the fibres

To complete the stress analysis of the ears 7 different load cases were applied to analyse the influence of misalignment of the fibres on the stresses in the ears. The different load cases are shown in Table 3.2. The first load case is an ear with well-aligned fibres that have 7 mm of stock. In the 2nd load case on fibre has an off-set to the side. The 3rd load case has a 5 degrees up and down angle offset of the fibres with the same length of stock still. As it appeared the worst load case was fibres angled to the side. The 4 remaining load cases cover this, for different lengths of stock and for a smaller angle as well. The different lengths of stock were simulated to account for a possible change in stock length to accommodate holding it for welding, but also for reaching the correct suspension dynamics.

Table 3.2 Seven different load cases for ears with misaligned fibres

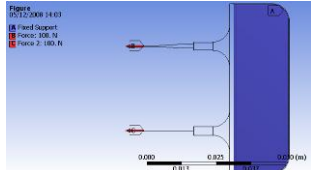
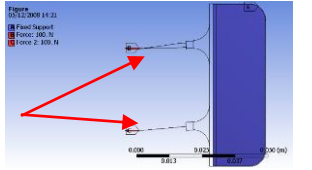
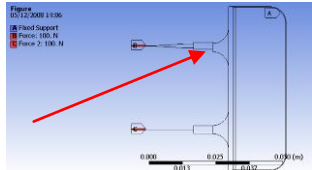
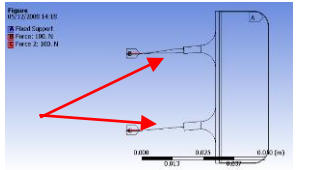
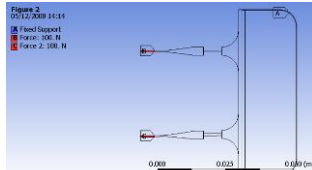
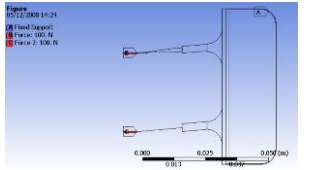

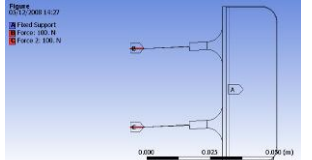
<p>1</p>  <p>Well aligned fibres, 7 mm stock</p>	<p>4</p>  <p>5° angle to the side, 3 mm stock</p>
<p>2</p>  <p>One fibre off-set by 1 mm in z, 7 mm stock</p>	<p>5</p>  <p>5° angle to the side, 7 mm stock</p>
<p>3</p>  <p>5° angle up and down</p>	<p>6</p>  <p>5° angle to the side, 10 mm stock</p>
<p>7</p>  <p>2.5° angle to the side, 7 mm stock</p>	<p>7</p>  <p>2.5° angle to the side, 7 mm stock</p>

Table 3.3 Stresses calculated using FE analysis of the different load cases shown in Table 3.2

Model/Description	Max stress 1 mm into horn [MPa]	Max stress 3 mm into horn [MPa]	Max shear stress at bond [MPa]	Max normal stress at bond [MPa]	Min principal stress [MPa]
Well aligned fibres, 7 mm stock	9.6	4.2	0.7	1.0	-3.2
1 fibre offset by 1 mm, 7 mm stock	24.0	8.0	0.6	0.7	-4.2
Fibres at 5° angle up down, 7 mm stock	27.4	7.0	1.3	0.8	-4.1
Fibres at 5° to side, 3 mm stock	53.0	20.0	1.0	0.7	-3.0
Fibres at 5° to side, 7 mm stock	49.8	10.6	1.0	0.7	-3.2
Fibres at 5° to side, 10 mm stock	65.0	21.0	1.0	0.8	-3.3
Fibres at 2.5° to side, 7 mm stock	37.1	10.3	0.7	0.8	-2.8

When looking at the results in Table 3.3 one can see that the shear and normal stresses at the bond and the minimal principal stress (which is the maximum compressive stress acting at the edge of the bond nearest the weld horns) do not change significantly as a function of the misalignments. The stresses in the weld horns do change significantly though. As the stresses in the connection between the fibres and the weld horns in the finite element modelling are not real due to small discontinuities the maximum stress 1 mm and 3 mm into the weld as seen from the tip of the weld horn has been taken. Results show that the stresses for side angled fibres increase more quickly than fibres angled up or down. In order to avoid increase to 25 MPa (50% of the average strength of silica) the angular off-set of the fibres should be limited to less than 1° in the case of the stock length being 10 mm.

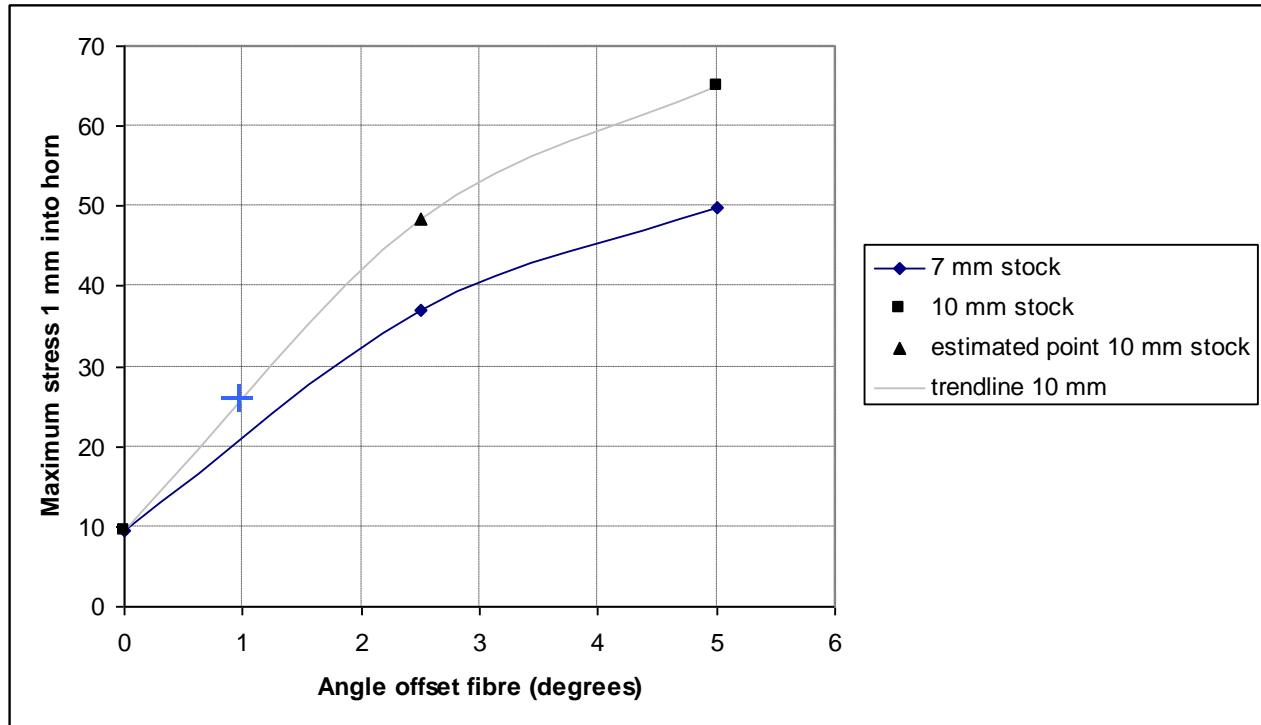


Figure 3.4 Derivation of maximum angle off-set allowed for a maximum stress of 25 MPa using FE data of the maximum stress 1 mm into the horn as taken from table 3.3.

3.3 Weldability

The weld process of the ears as will be explained in more detail in section 5.2 requires an even heating of the fibre stock and the weld horn of the ear on all sides. The heating is done by heating the end of the stock and the weld horn with a CO₂ laser beam of 3 to 5 mm in diameter. The fronts of the stock and the horn have easy access as there is no material obstructing beam access. However the side of the horn that is closest to the ITM/ETM test mass or PUM mass is obstructed by it. To allow the beam to access all parts of the weld area a mirror is used to reflect the beam onto the rear of the weld horn and stock. This mirror has certain minimal dimensions and the distance of the centre of the weld horn from the side of the test mass was chosen based on a minimal practical size of this mirror and reflection of the beam onto it.

The distance of the centre of the weld horns to the flat of the optic was chosen to be 7 mm. The decision on this 7 mm was based on experiments conducted during November 2008 and based on initial CAD drawings of mirrors that would make sure the CO₂ laser beam would access the whole welding area (discussed on slide 13 of T080338-v1 and shown in Figure 3.5). In a large sequence of experiments after the test ears were manufactured the design of the welding mirrors was refined, a welding procedure was established and the weldability and strength of the welds were proven (see the discussion in 5.2).

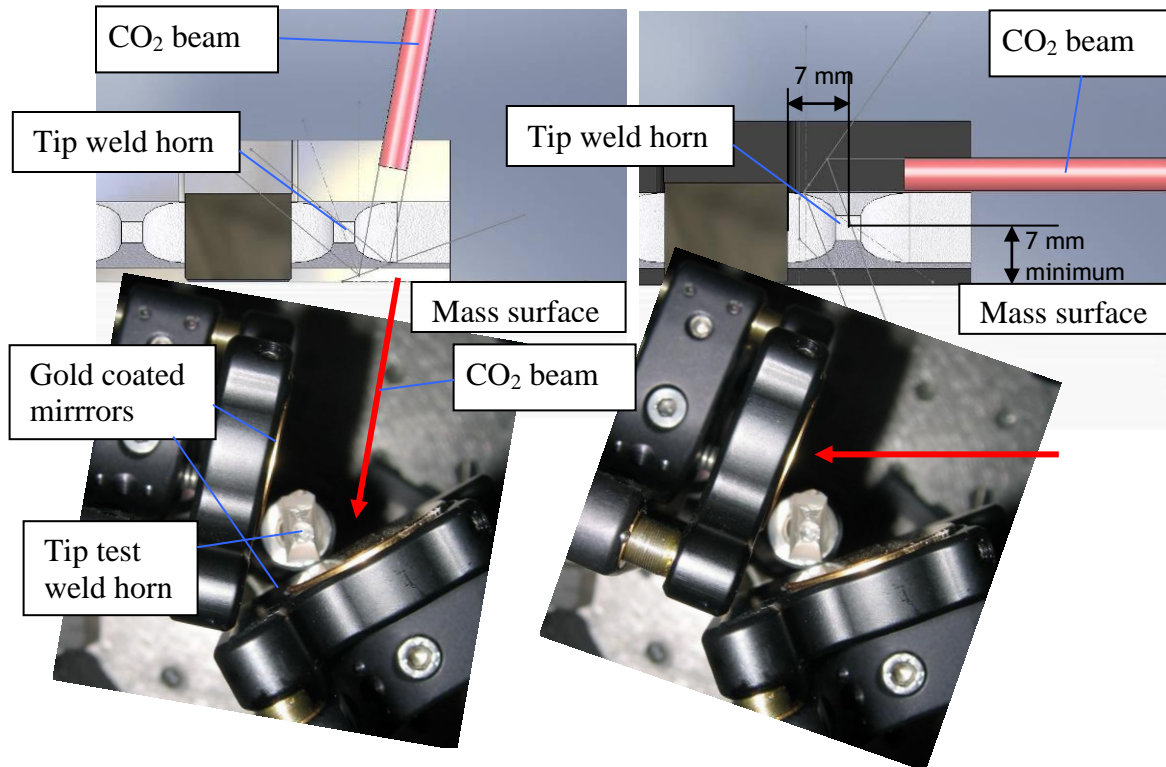


Figure 3.5 Images of initial tests and CAD drawings to determine welding access. In the top two images the CAD drawings show beams coming from 2 sides and some grey lines outlining where gold coated mirrors could be. In the bottom two images the beams are drawn as applied in an experimental set-up of two gold coated mirrors with a test weld horn (old GEO horn) on an optical post to test welding with mirrors in place at appropriate angle. In later stages of the project the welding technique has evolved to welding from 1 direction with one mirror. The beams still comes from the same direction as in the top left image.

3.4 Location of the ear and suspension dynamics

For the suspension dynamics it was important to ensure that the flexure point of the fibres and the steel wires could be at the right location. The location of the flexure points is defined in T080096-v1. Furthermore the relation between the physical position of parts and the flexure points is discussed in T070138-01 and M080134 states the latest locations of the effective flexure points for the suspension wires of the PUM (d_2) and the suspension fibres (d_3 and d_4) on the PUM and ETM/ITM. The latter states $d_2 = 10$ mm above COM, which places the physical position of the top of the wire break-off prism at 7.2 mm above the COM. The effective flexure point of the fibre on the PUM should be $d_3 = 1$ mm below the COM and for the fibre on the ETM/ITM it should be $d_4 = 1$ mm above the COM. This situation is shown for the PUM in Figure 3.6. Assuming that the minimal distance between the ear and the edge of the prism in vertical direction should be 2 mm, the minimal length of the fibre stock plus neck up to the flexure point has to be $10 + 1 = 11$ mm (see Figure 3.6 or Figure A.1 in Appendix 1). The maximum available length the fibre stock plus neck up to the flexure point for the stated distances is governed by how close the ear can be moved to the edge of the bonding flat. The top edge of the ear cannot be less than 5 mm from the edge of the bonding flat, because of steep roll-off due to polishing. The maximum available length of the stock plus neck up to the flexure point is therefore $11 + 5 = 16$ mm (Figure A.2 in Appendix 1).

There are other solutions existent that give very comparable dynamic behaviour of the suspension. the dynamics requirements as stated in a document written by Ken Strain (T0900556-v1). Here $d_2 = 0.3$ mm and d_3 and d_4 are 7.2 mm, which gives a lowest pitch frequency of 0.50 Hz. When considering this case the minimal length of the stock plus neck is $4 + 7.2 = 11.2$ mm (Figure A.3 in Appendix 1) and the maximum distance is $15 + 7.2 = 22.2$ mm (Figure A.4 in Appendix 1).

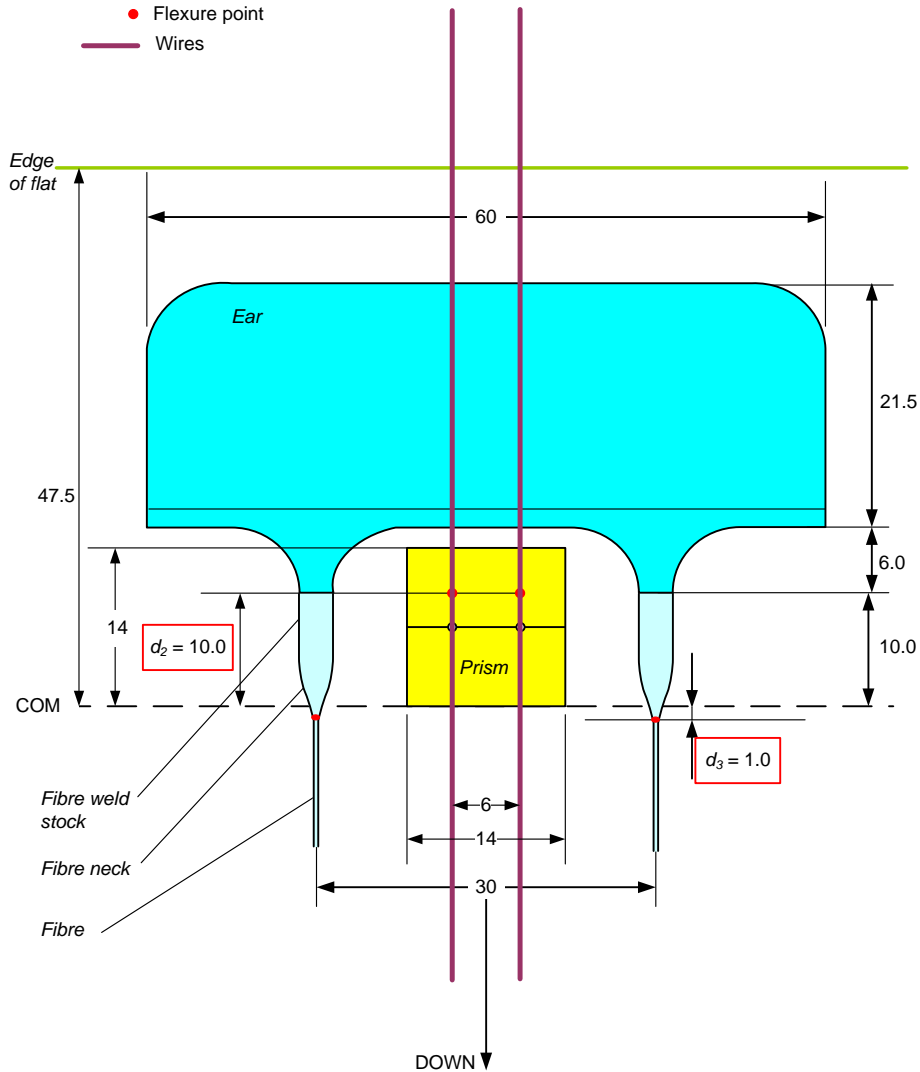


Figure 3.6 Position of the prism, ear, wires, fibres and effective flexure points on the PUM relative to the COM and the top edge of the flat.

Ideally the total length of the stock plus neck is minimised to reduce the amount of strain energy moving away from the flexure point region. However, practically speaking, the stock and flexure have a minimum length, because the neck cannot be made shorter than 6.7 mm on one side and 7.5 mm on the other side. The difference between those is determined by the pulling programme. Also, a minimum of 10 mm of stock length is needed to be able to hold the fibre into place during welding (internal e-mail communication A.V. Cumming to K. Strain 17/07/09). This makes the current practically achievable length of fibre stock plus neck up to the flexure point 16.7 to 17.5 mm.

In the current status of development of fibres it is therefore not possible to maintain the d-distances of $d_2 = 10$ mm and $d_3 = 1$ mm. However, because it is close and fibre optimisation work is ongoing both options are still under consideration at this point.

3.5 Hydroxide catalysis bonding

Hydroxide catalysis bonding is the baseline technique used for joining the ears to the flat sides of the PUM and the ETM/ITM. This technique involves applying a very small amount of an alkali sodium silicate solution in water onto the silica flat and then placing the ear on top of it. The hydroxide solution lightly etches the surface of both the flat and the ear to free up silica to form silicate chain connections between both surfaces. This technique was used in GEO600 to suspend the test optic via silica “ears” on silica fibres (see Figure 2.2).

A large number of studies were done to determine the strength of silicate bonds (collated in T080343). The baseline bonding solution to be used is a 1:6 volume ratio of commercial sodium silicate solution (10% sodium hydroxide, 27% SiO₂) to DI water. The lowest strength reported for bonds made with this specific solution was 1.45 MPa (Elliffe et al. 2005). This is a factor of ~9 above the required nominal shear stress that will be applied to the proposed ears. Additionally, all other research indicates the actual strength of the hydroxide catalysis bonds is higher than the value above. In recent strength measurements average strengths of 16 MPa were measured (Karen Haughian).

Experiments with hydroxide catalysis bonding of the test batch of ears have been performed and the bonds have been subjected to high loads. These experiments are discussed in sections 5.1 and 5.2.

3.6 Thermal noise of the bonds

The thermal noise associated with the hydroxide catalysis bonds between the ears and the ITM/ETM test masses and penultimate masses is discussed in detail in P0900053-v2 (Physics Letters A, 374 (2010), 3993-3998). The thermal noise contribution of the bonded ear at a frequency 100 Hz is required to be less than $7 \cdot 10^{-22}$ m/ $\sqrt{\text{Hz}}$. In summary the referenced document discusses the calculation of the thermal noise associated with the bonded ears by using FE analysis to calculate the strain energy density following from the elastic deformation of the test mass suspended on ears driven by an oscillating Gaussian pressure with a peak force magnitude of 1 N. From that the average power dissipated can be calculated and using the Fluctuation Dissipation Theorem the thermal noise can be calculated, based on experimental values for the mechanical loss of the bonds and based on a range of bond thicknesses up to 90 nm. The referenced paper shows that the calculated thermal noise arising from the bonded ears is $6.6 \cdot 10^{-22}$ m/ $\sqrt{\text{Hz}}$ in the worst case.

It has been suggested that a non-Gaussian "crackle" noise or 'glitches' could arise from the bond interfaces under the suspension load, which would limit detector sensitivity. In P0900310 (Class. Quantum Grav. 27 (2010) 155017 (13pp)) the fibre violin mode amplitude of several days of GEO600 detector strain measurements, was monitored for glitches to see if any evidence of this 'crackling' noise could be found. No excess noise above what was considered to be thermal noise was observed.

At UT Brownsville research is ongoing to develop an experiment that can measure the creep rate of aLIGO hydroxide catalysis-bonded silica ears (see G1301160).

3.7 Thermal Noise contribution from material loss of the fibres

The projected loss of the fibres was calculated through FE analysis of the strain energy involved in a single optimised dumbbell-shaped fibre (designed to minimise the thermoelastic loss contribution so it is no longer dominant) suspending a 10 kg mass (Figure 3.7) and analysing the deformation of the fibre when considering the pendulum mode only (see P0900084-v2 for a detailed discussion). The shape and length of the fibre necks was varied in these analyses. Using the techniques outlined in P0900084-v2 the surface, bulk and thermoelastic losses were calculated, together with the pendulum mode dilution factor, which was calculated from a 4 fibre model. It was shown that though use of optimised fibres, the total mechanical loss occurring in the pendulum mode was meets the suspension thermal noise requirements (T080091-00). The optimised fibres push the residual thermo-elastic loss peak well below 10 Hz, out of the detection band.

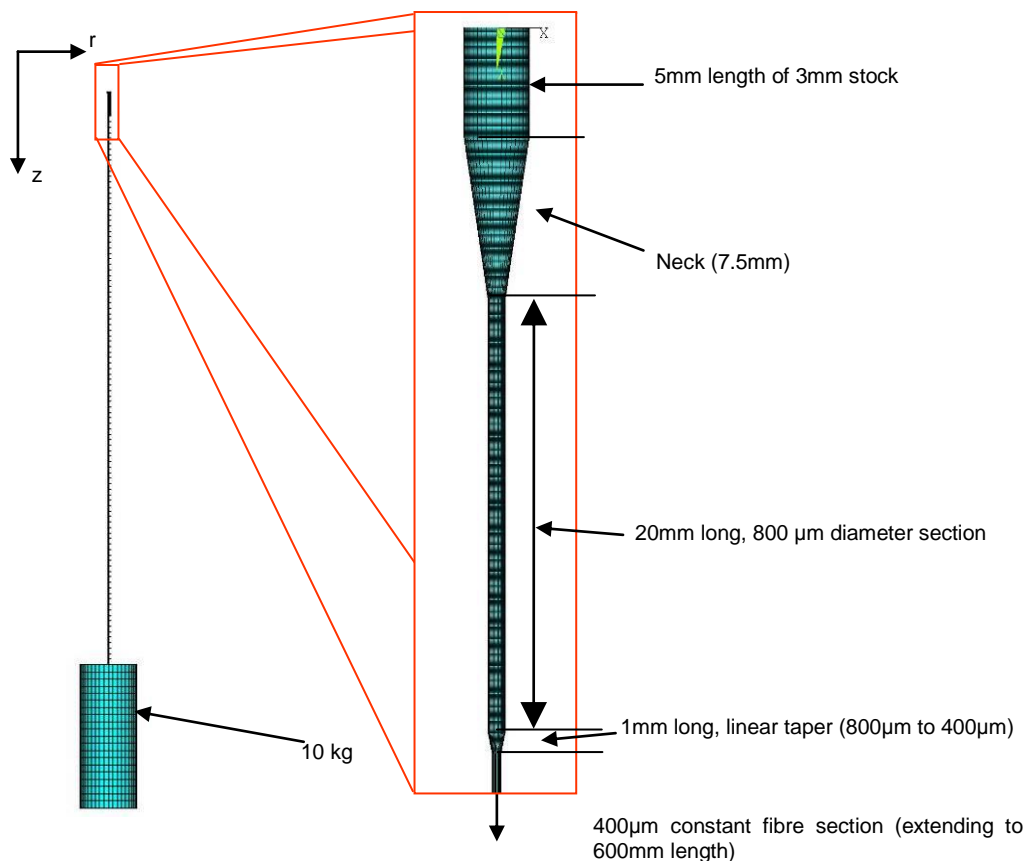


Figure 3.7 FE model used to evaluate the pendulum mode fibre deformation, for analysis of the pendulum mode mechanical loss of fibres.

4 Fabrication procedure

The drawings of the ETM/ITM ears and the PUM ears are D080571-02 and D090007-00.

The manufacturing procedure consists of three main parts and is performed by two vendors:

- in the first part the shape of the ears is cut, machined and inspection polished using a mechanical process over its entire surface by vendor 1 and 2.
- in the second part all surfaces except the bonding surface of the ear are flame polished by vendor no. 2.
- in the final stage the bonding surface is polished to a flatness of $\lambda/10$ (over 95% of the surface @ $\lambda = 633 \text{ nm}$) by vendor no. 1.

The flame polishing step has been introduced into the process in order to ensure that micro-cracks in the ear surface (particularly in the weld horns) are sealed, thus reducing the likelihood of having an ear that has a low strength because of this.

The base material is 62 x 30 x 28 mm Suprasil 312 (Heraeus) blocks. Two ears can be cut from each block as shown in Figure 4.1. The three stages of production are discussed in brief bullet points in section 4.1 to 4.3.

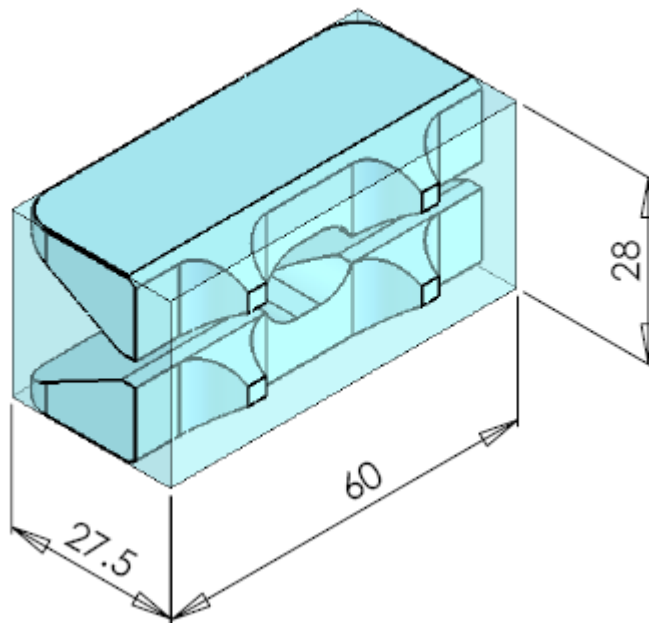
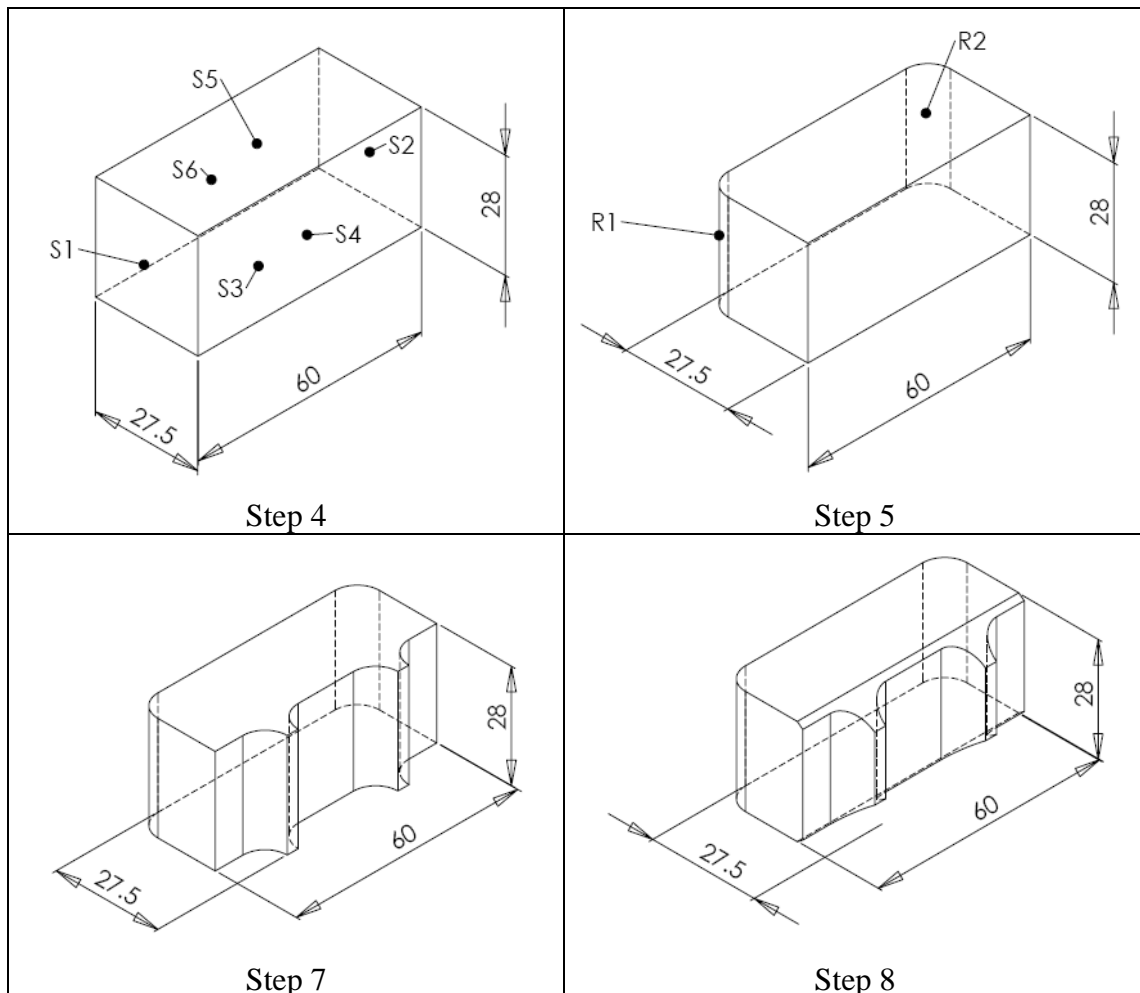


Figure 4.1 Arrangement of two ears in one block

4.1 Shaping of the ear

1. Stack parts
2. Hand grind 90 deg angle
3. Block & smooth stack
4. Polish four sides (bonding surfaces (S3 and S5), sides (S1 and S2), tip of the horns (S4) and top edge (S6), see Figure 4.2)

5. Polish the radius at the rounded top edges (R1 and R2) (see Figure 4.2)
6. De-stack
7. Machine the radiused parts of the weld horns for 2 ears (see Figure 4.2)
8. Machine the underside of the ear weld horns (see Figure 4.2)
9. Slice the part to form two ears (see Figure 4.2)
10. Polish the top ledge
11. Block and mill the top face (see Figure 4.2)
12. Smooth polish the top face
13. Block and mill the top side of the ear weld horns
14. Smooth polish the top side of the ear weld horns
15. For the PUM ears machine the notch in the top of the ear (see Figure 4.2)
16. For the PUM ears polish the notch in the top of the ear
17. Polish chamfers



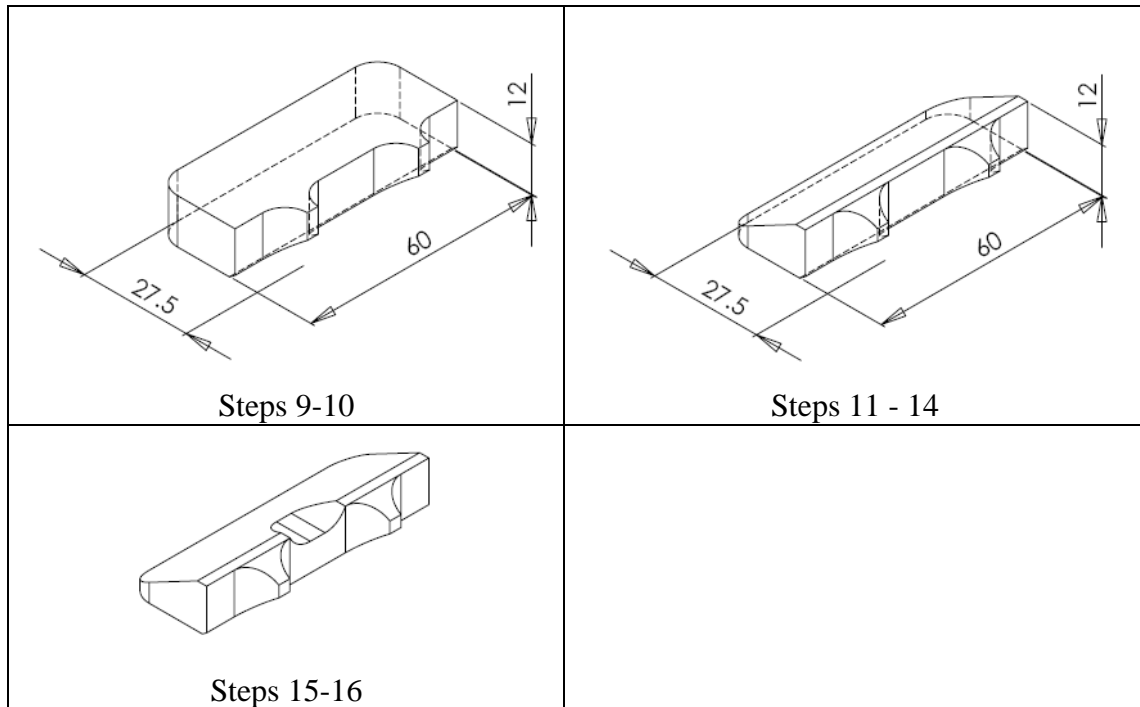


Figure 4.2 Visualisation of steps in the shaping process of the ears

4.2 Flame polishing

- The ears are cleaned in a 19 VOL% solution of HF in water.
- The ears are placed on top of a ground quartz plate into a quartz enclosure with filtered air
- Using a small burner with a silica nozzle and a hydrogen oxygen flame, the edges and surfaces (except the bonding surface and its edges) are flame polished
- The ears are placed into an annealing oven after flame polishing. They are annealed at 1120 °C for 2 hours with a slow cooling down process overnight.

4.3 Polishing of the bonding surface

- 6 ears are blocked onto a plaster block
- The flats are lapped to a flatness of 300 to 400 nm.
- Remove the ears from the plaster block
- Each ear is individually UV bonded onto a blank for magneto-rheological figuring (MRF)
- MRF (in a two stage iterative measurement – figuring process)
- De-bond the ear and test
- Rework as required.

5 Tests performed

5.1 Hydroxide catalysis bonding

Up to this date (1/11/2009) a total of 26 ears of the test batch of ears have been bonded onto silica disc inserts in aluminium plates using hydroxide catalysis bonding.

16 ears were bonded onto the discs using jigs that were made specifically for the discs insert plates. 8 ears were bonded with the newly designed bonding jig that will also be used for bonding the ears to the masses at LASTI (and Advanced LIGO).

In all cases the bonding solution consisted of 1:6 volume ratio of commercial sodium silicate solution (10% sodium hydroxide, 27% SiO₂) to DI water was used. The solution was mixed by thoroughly shaking it, then filtering it using a 0.2 µm medical filter and finally centrifuging it.

In all cases the discs and ears were cleaned thoroughly by rubbing with cerium oxide for about 2 minutes using an optical cloth wetted with DI water, followed by a rubbing clean with bicarbonate of soda for about 2 minutes using an optical cloth wetted with DI water. They were then rinsed with DI water. Finally the discs and ears were rinsed with methanol.

Just before commencing the bonding, the ears and discs were inspected for dust specks using a high intensity light source with fibre spot light at high power and wiped with methanol.

In all but one case an amount of 9.6 µl of bonding solution (equivalent to 0.8 µl/cm²) was pipetted onto the disc for bonding (in GEO an equivalent of 0.4 µl/cm² was used). In one case 4.8 µl of solution was used. However, in this case the bonding solution did not willingly cover the entire bonding surface and after curing only half the surface area was bonded successfully.

3 of 26 ears showed bonds that were partially not bonded properly, shown by coloured fringes in the bond. In one of the cases 4.8 µl of solution was used, which is deemed not to be enough for a large bonding area like is the case for the ears. In one of the cases the flatness of the ear was very poor. In the third case the reason for the low quality bond is unknown.

5.2 Weldability and strength tests

5.2.1 Welding procedure

In a large sequence of experiments the welding procedure for welding fibres onto the weld horns of a test batch of ears was developed. In this procedure described in T0900391 the 3 mm diameter stock ends of the fibre are held with zirconia tipped tweezers in a fibre holder. A photograph of the welding set-up is shown in Figure 5.1. The tweezer tips can be manually manipulated with x-y-z stages. The fibre ends are brought in butt contact with the weld horns. A custom designed gold coated mirror is placed behind the fibre stock and the ear weld horns to allow the CO₂ beam to be reflected onto the rear surfaces. This ensures that a uniform weld can be achieved. The CO₂ beam is scanned over the complete weld area to heat up the stock and weld horn. When the material is hot enough and its viscosity reduces significantly (the material starts to melt), the stock material is fed towards the horn using the manipulators to allow the weld to form.

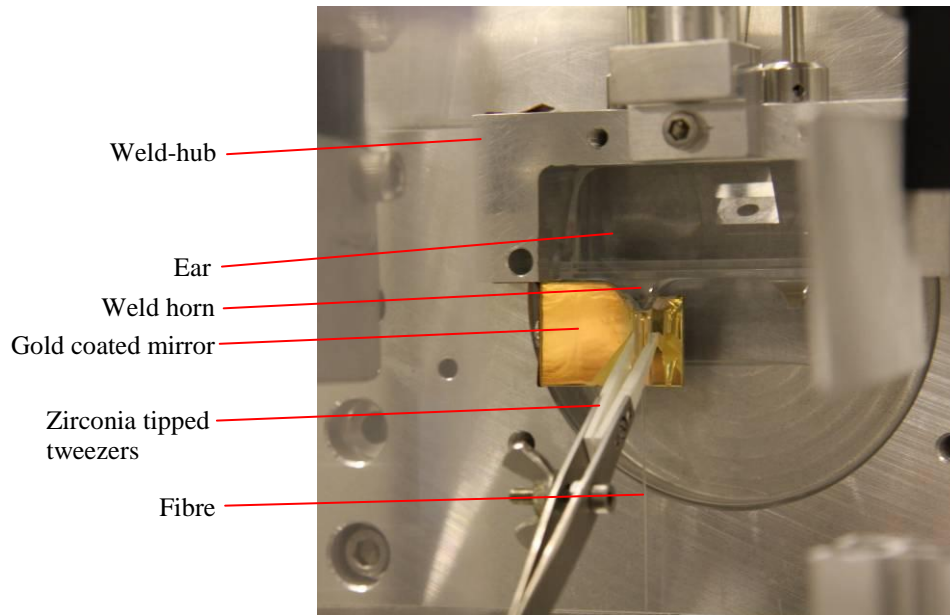


Figure 5.1 Image of zirconia tipped tweezers holding a fibre against one weld horn of an ear on a disc insert plate. A gold coated mirror is held behind the weld horn to allow heating with the CO₂ beam around the entire weld location. The gold-coated mirror is attached to the weld hub, which is the aluminium piece sitting around the ear.

The procedure also includes a de-stress scheme after the zirconia tweezers have been removed. In this de-stress the fibres are put under slight tension and the weld area and the stock are gently heated to relieve thermally induced stresses during the welding and to align the welded stock with the direction of tension.

5.2.2 Double fibre cartridge tests

8 strength tests to destruction have been performed on cartridges in which 2 fibres were welded between two test ears. The cartridge with welded fibres can be seen on the left in Figure 5.2. On the right a snapshot is shown of a video taken during one of the strength tests. The minimal load required for the welds is 22 kg (10 kg per fibre + 10% overload). The results for the 8 cartridge tests that were performed all showed a strength above this value (see Table 5.1). For the two tests (1 and 4) that show the lowest strengths an explanation exists. So nominally all other tests showed a safety factor of at least two, which means the weldability of the ears has been proven through these tests.

Tests 7 and 8 were carried out with a fan blowing above the welding set-up to mimic airflow variations to see if that would affect the weld or fibre strength as there were concerns that this could be a possible reason for reduced strength of monolithic suspensions. Both values fall within the bandwidth of the other strength tests. There is therefore no indication that the strength is reduced due to higher airspeeds in the laboratory area.

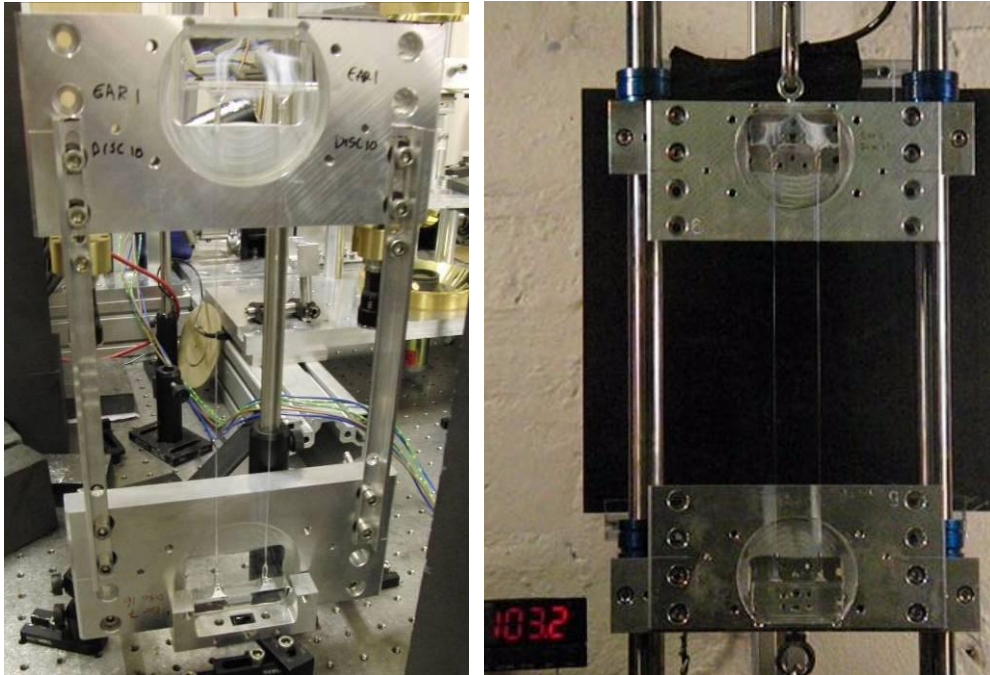


Figure 5.2 Cartridges with two fibres welded in between two ears on the optics table on the left and in the strength tester under a load of 103.2 kg on the right

Table 5.1 Strength test results of double fibre cartridge tests

Test	Remarks	Strength [kg]
1	June, one fibre touched by tweezers	24
2	June	40
3	June	100.1
4	September, training, poor looking welds	28
5	September, still air	58.5
6	September, still air	103
7	September, fan	40.6
8	September, fan ½ speed	83

5.2.3 Full test suspensions

As additional proof of the weldability of the ears, 3 successful full 4 fibre test suspensions of a 40 kg aluminium dummy mass have been achieved in Glasgow. These suspensions were all subjected to vibrations test to determine different dynamic modes. Most of these modes were excited by hitting the suspended mass with a mallet. Photographs of the 1st of the successful test suspensions are shown in Figure 5.3. In the third suspension an overload test was performed successfully. In this test the nominal load (10 kg per fibre) was increased by 25%. Each fibre was taking 12.5 kg.

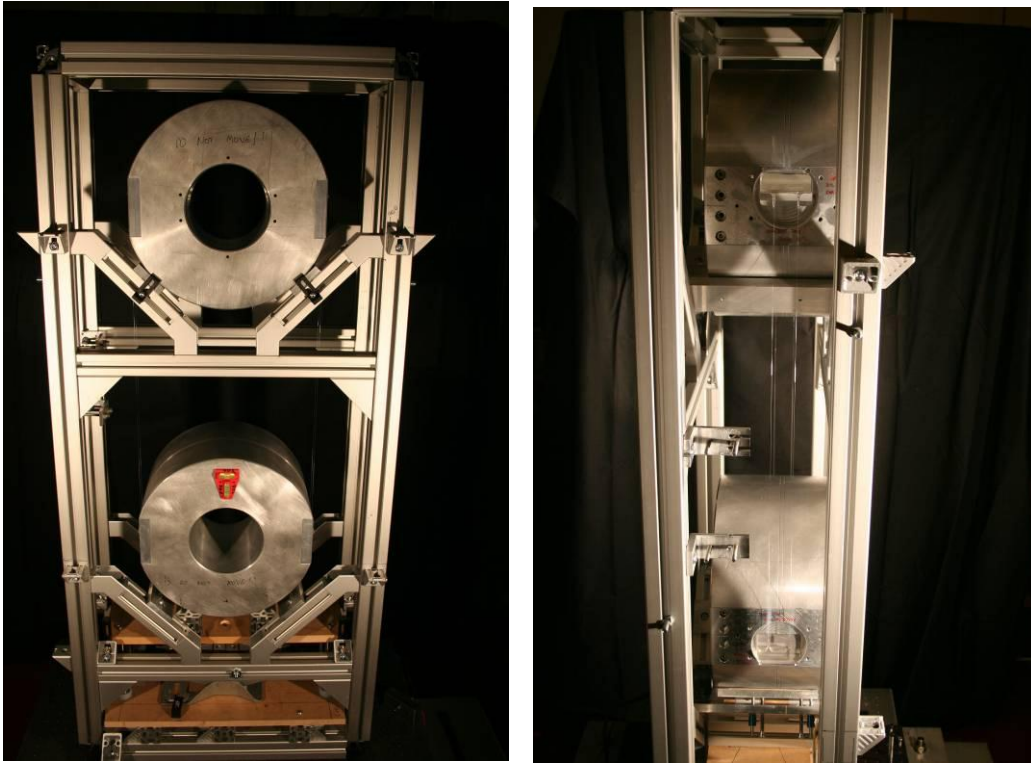


Figure 5.3 Photographs of the first successful 40 kg test suspension in Glasgow

5.2.4 Bond quality

Of the 26 ears that have been bonded using hydroxide catalysis bonding 16 ears have been subjected up to now to at least the nominal load on at least one occasion. One of these ears was the ear with the poor looking bond of 4.8 μl of solution. 8 of the 16 ears have been subjected to two tests and 6 of those have been loaded to destruction in a double fibre cartridge test. No changes have been observed in the quality of the bonds between the ears and the disc inserts in any of the suspension tests.

5.2.5 Weld horns

A total of 29 ears have been subjected to at least one suspension and/or double fibre cartridge test (T0900557-v1 contains the test records). 11 ears have been subjected to two tests. They have been reused by removing the remaining bit of the fibre using a diamond scribe and breaking it off, followed by a light grind with a diamond grinding tool and a light flame polish.

Two of these 29 ears were lost in the double fibre cartridge test that went up to 103 kg (ears 16 and 18). The ears were shattered, though the bonds were still intact.

Three of 29 ears have lost one full horn (ears 4, 6 and 56 respectively). All of these were lost in double fibre weld tests that had a load of more than 280% of the nominal load. They broke at 100 kg, 58 kg and 62 kg respectively.

5 horns on 4 ears (ears 8, 13, 15 and 18) have been chipped after breaking suspensions (1 per suspension). The horns of these ears are considered to be reparable and it is therefore possible to

weld new fibres to them. Tests are currently ongoing to optimise flame polishing/welding techniques to do this.

Based on the current experience the most likely moments of failure of the suspension are:

- 1) Failure of a fibre during initial loading of the suspension before moving the structure into the tank. The maximum load will be 11 kg per fibre under these circumstances due to an overload test that is scheduled to be conducted.
- 2) Failure of a fibre during loading of the suspension just before closing the vacuum tank. The maximum load will be 10 kg per fibre under these circumstances.

The most likely reason for a fibre failing in these cases would be unintentionally having touched a fibre in the processes before welding and during operations to connect the chains and moving the structure into the vacuum tank.

Risks are reduced by implementing a proof test of the fibres just before welding and a policy of replace-when-in-doubt. To reduce the risk of touching fibres in ongoing operations, a fibre guard will be fitted after initial suspension.

A full weld horn failure in these cases is considered to be unlikely. It is likely that one of 4 ears will have a chip in one of the weld horns, which is considered to be reparable.

6 Conclusions

A design of an ear for the attachment of fibres to the ETM/ITM test mass and to the penultimate mass has been presented. A range of finite element analyses has been performed in the design phase to prove noise performance will meet requirements. The ear will fit and will not interfere with any other parts of the suspension. A test batch of 58 ears was produced. A large number of these ears have been used and reused successfully in bond and weld tests and test suspensions. It has been shown they are strong and that they can be used again. They have proven their strength and have therefore shown suitability and readiness for production for Advanced LIGO.

Advanced LIGO will have a total of 12 quadruple suspensions (plus 4 spare). In each of these suspensions there will be 4 ears (2 PUM ears and 2 ETM/ITM ears). This means a minimum of 64 ears will be needed. The Advanced LIGO UK project will provide 80 ears to Advanced LIGO.

Appendix 1

See below the four figures showing the available range for the fibre stock plus neck length for the two discussed combinations of d-distances.

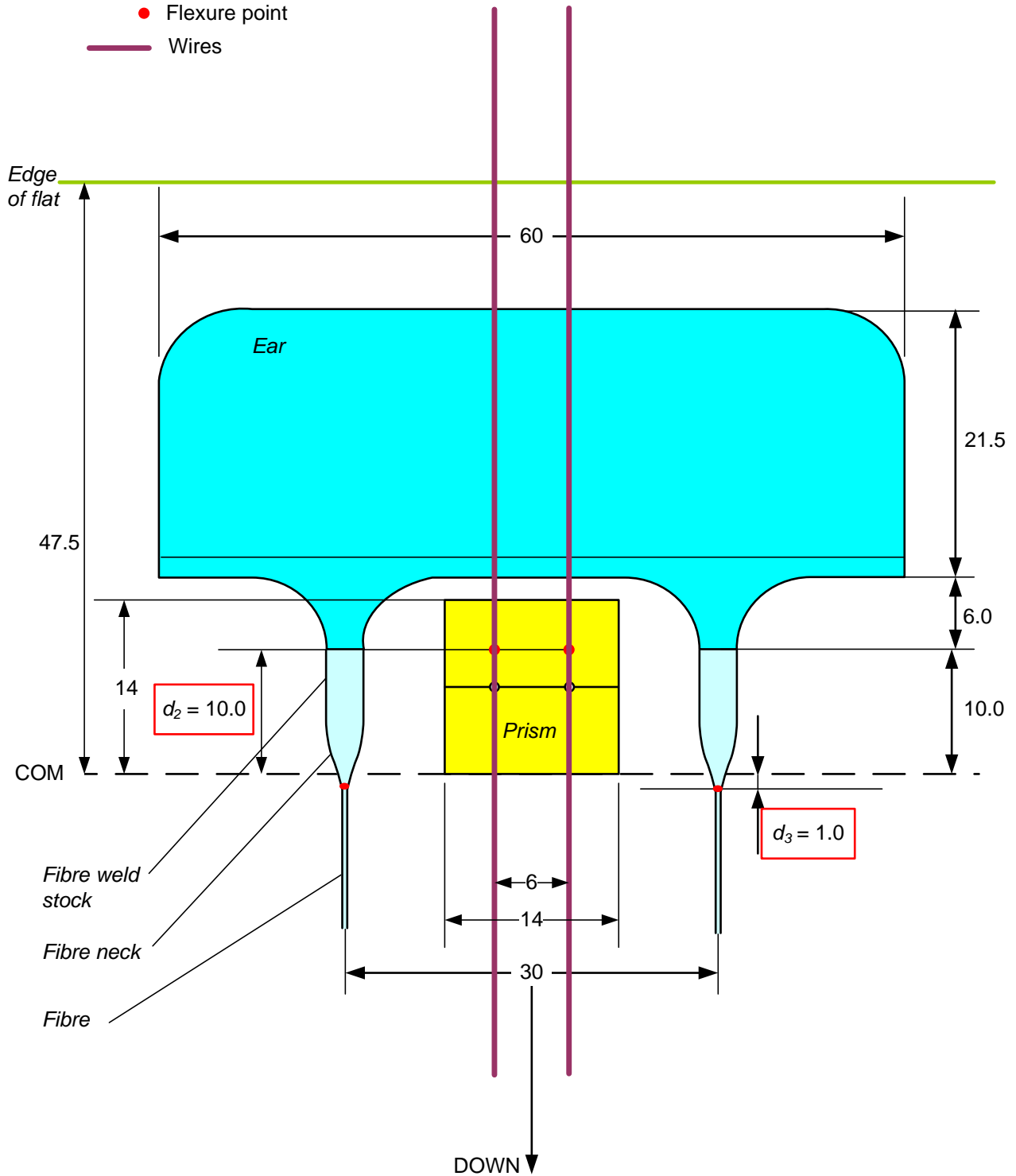


Figure A.1 Minimum stock plus neck length of 10 + 1 = 11 mm for d-distances $d_2 = 10.0$ mm and $d_3 = 1.0$ mm

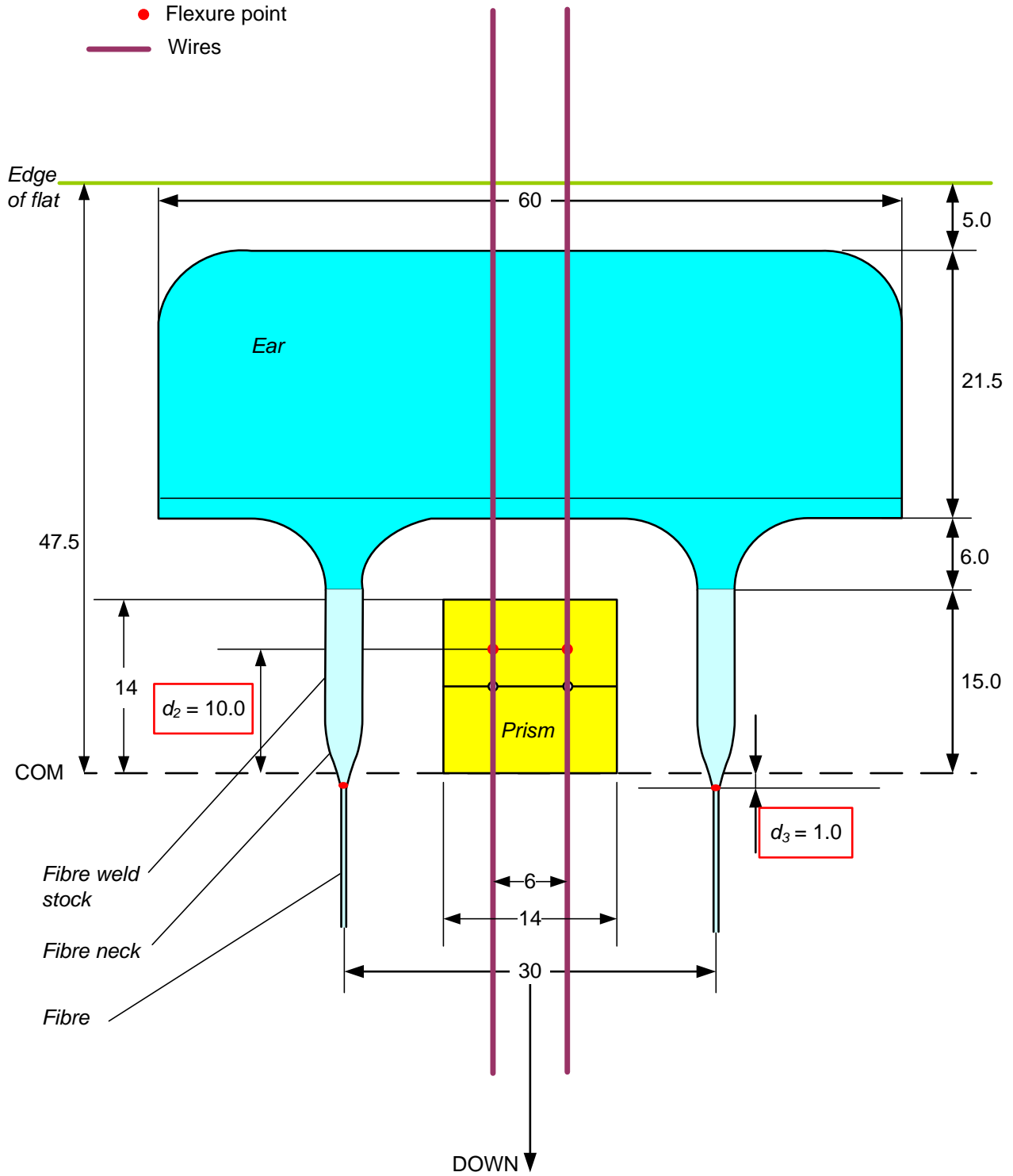


Figure A.2 Maximum stock plus neck length of $15 + 1 = 16$ mm for d-distances $d_2 = 10.0$ mm and $d_3 = 1.0$ mm

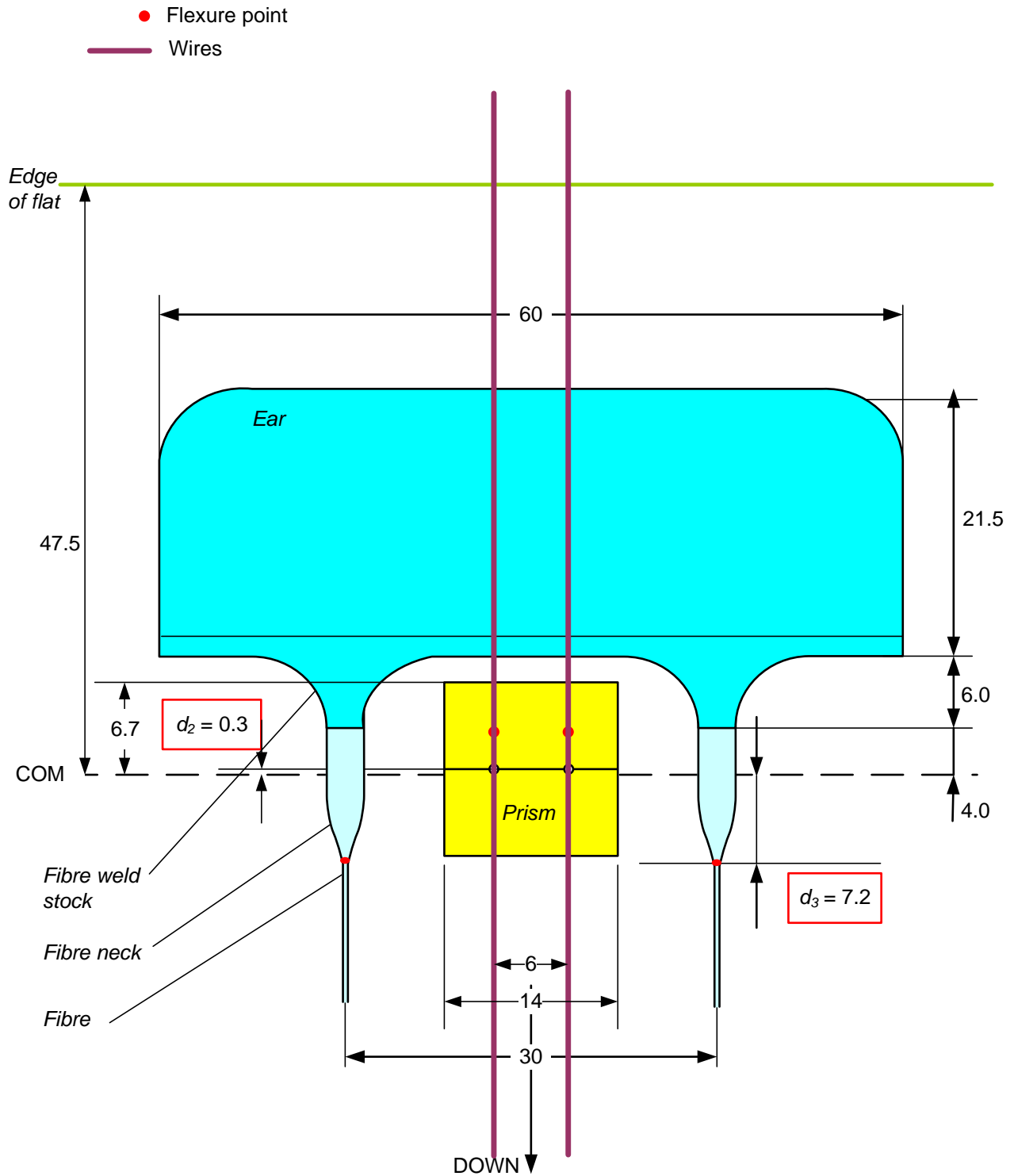


Figure A.3 Minimum stock plus neck length of $4 + 7.2 = 11.2$ mm for d-distances $d_2 = 0.3$ mm and $d_3 = 7.2$ mm

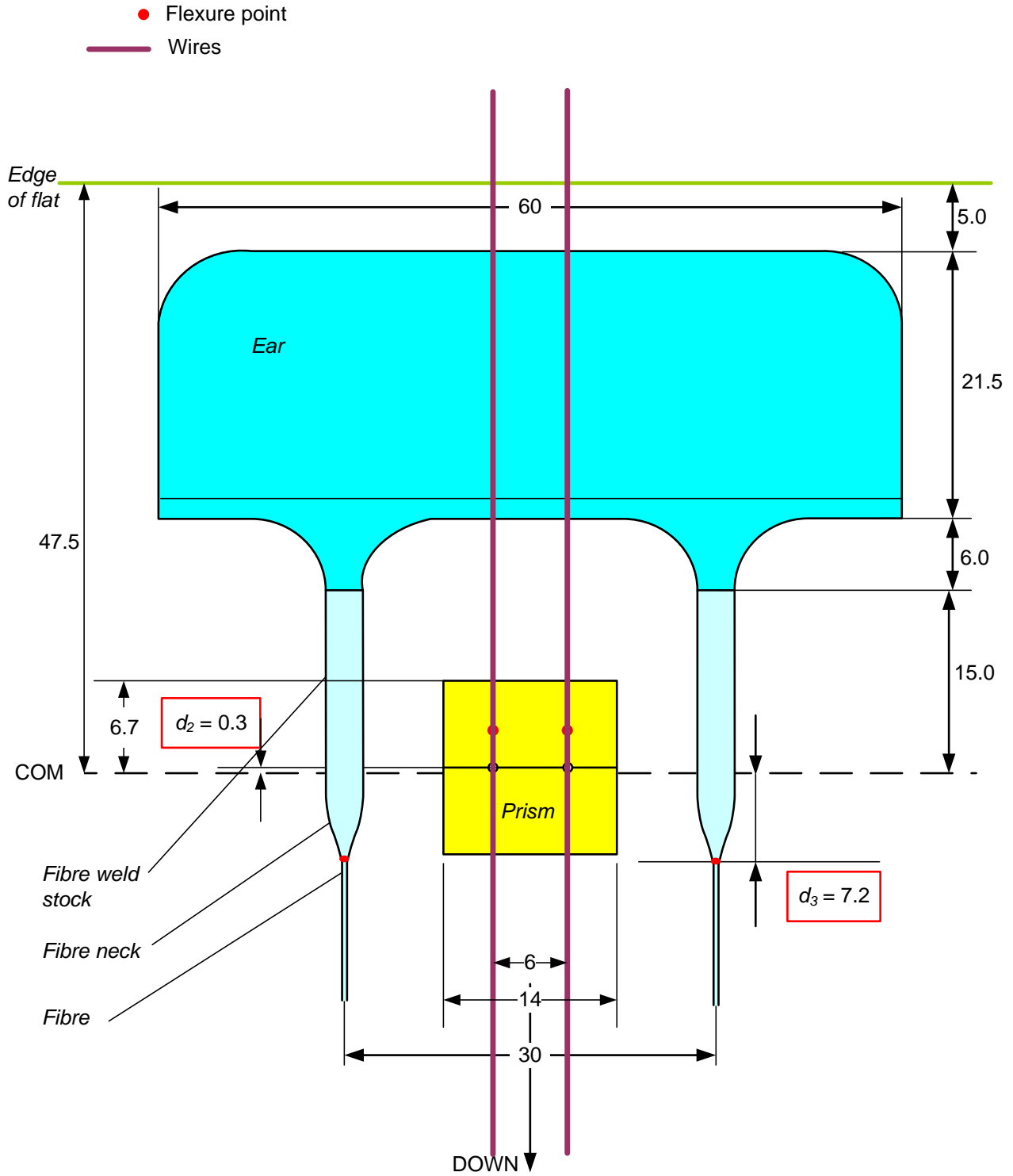


Figure A.4 Maximum stock plus neck length of $15 + 7.2 = 22.2$ mm for d-distances $d_2 = 0.3$ mm and $d_3 = 7.2$ mm